Comparative Medicine
Copyright 2010
by the American Association for Laboratory Animal Science

Vol 60, No 3
June 2010
Pages 225–232

# Mapping the Anatomy of Respiratory Syncytial Virus Infection of the Upper Airways in Chinchillas *(Chinchilla lanigera)*

**Jessica L Grieves,[1-3] Joseph A Jurcisek,[1] Brian Quist,[1] Russell K Durbin,[2] Mark E Peeples,[2] Joan E Durbin,[2] and Lauren O Bakaletz[1,*]**

**Although most viral infections of the upper respiratory tract can predispose to bacterial otitis media, human respiratory syncytial virus (HRSV) is the predominant viral copathogen of this highly prevalent pediatric polymicrobial disease. Rigorous study of the specific mechanisms by which HRSV predisposes to otitis media has been hindered by lack of a relevant animal model. We recently reported that the chinchilla, the preferred rodent host for studying otitis media, is semipermissive for upper-airway HRSV infection. In the current study, we defined the anatomy and kinetics of HRSV infection and spread in the upper airway of chinchilla hosts. Chinchillas were challenged intranasally with a fluorescent-protein–expressing HRSV. Upper-airway tissues were recovered at multiple time points after viral challenge and examined by confocal microscopy and immunohistochemistry. HRSV replication was observed from the rostral- to caudalmost regions of the nasal cavity as well as throughout the Eustachian tube in a time-dependent manner. Although fluorescence was not observed and virus was not detected in nasopharyngeal lavage fluids 14 d after infection, the latest time point examined in this study, occasional clusters of immunopositive cells were present, suggesting that the nasal cavity may serve as a reservoir for HRSV. These data provide important new information concerning the time course of HRSV infection of the uppermost airway and suggest that chinchillas may be useful for modeling the HRSV-induced changes that predispose to secondary bacterial infection.**

**Abbreviations:** HRSV, human respiratory syncytial virus; rrHRSV, recombinant red fluorescent human respiratory syncytial virus; URT, upper respiratory tract.

Human respiratory syncytial virus (HRSV), an enveloped, negative-strand, nonsegmented RNA virus of the family *Paramyxoviridae*, is the single greatest causative agent of acute respiratory tract infections in infants and children worldwide.[23] Although HRSV infection generally is limited to the upper respiratory tract (URT), in the United States, primary HRSV infection is associated with a 0.5% hospitalization rate for those children who develop severe bronchiolitis or pneumonia.[9] One of the most interesting aspects of HRSV is its ubiquity: there are annual winter–spring outbreaks in temperate climates,[5] and approximately 90% of all children have experienced infection by their second birthday.[9] Although immunity to HRSV is sufficient to prevent reinfection of the lower airway in most human patients, this response is incomplete, resulting in reinfection of the upper airway throughout life.[9] Although URT infection by HRSV alone does not constitute a serious problem for healthy adults, its association with the development of bacterial otitis media in children[11-13,17-19,21,25,28,29,34] and exacerbation of asthma in all age groups[16] make it an important health concern.

*Received: 05 Aug 2009. Revision requested: 05 Sep 2009. Accepted: 23 Jan 2010.*
*[1]Centers for Microbial Pathogenesis and [2]Vaccines and Immunity, Department of Pediatrics, The Research Institute at Nationwide Children's Hospital, and [3]Department of Veterinary Biosciences, The Ohio State University College of Veterinary Medicine, Columbus, Ohio.*
*[*]Corresponding author. Email: Lauren.Bakaletz@nationwidechildrens.org*

Despite the ubiquity of the virus, the epidemiology of HRSV is not well understood. There is no known animal reservoir, and although new strains emerge over time, many remain in circulation over several seasons or reappear many years after they were first detected.[27,33] Therefore, although antigenic variation driven by development of HRSV immunity in a given population is possible, this hypothesis has not yet been proven. In fact, in one study,[10] human subjects could be infected repeatedly with the same HRSV strain, and the presence of virus-specific antibody provided only short-lived and incomplete protection. Therefore, HRSV may circulate among seropositive persons, and it has been suggested that persistently infected persons may harbor the virus between seasonal outbreaks.[30,32] Therefore, in addition to the important clinical issues surrounding the prevention of HRSV disease, basic scientific questions regarding HRSV circulation and mechanisms of viral immunoevasion remain unanswered.

A key hurdle in the study of HRSV pathogenesis has been the lack of a suitable animal model. Most published studies have used BALB/c mice, which have the advantage of many reagents available for the study of immune responses but the disadvantage of relative resistance to HRSV infection.[22] Although pulmonary infection is easily detected in HRSV-infected mice, primary infection of the upper airway in this species is minimal[6,7] and secondary infection of the URT does not occur. More susceptible rodent species include the cotton rat (*Sigmidon hispidus*)[26] and chinchilla (*Chinchilla lanigera*),[6] which are both relatively permissive for

HRSV infection of the upper airway. Given the paucity of URT specimens encountered in general pathology practice, the development of a robust small animal model for the study of HRSV infection and spread in the uppermost airway is particularly important. Moreover, effective vaccine development depends on a better understanding of why this compartment remains susceptible to reinfection in immune hosts.

Here we describe the anatomy of HRSV infection in the chinchilla URT over a 2-wk period, using confocal microscopy to monitor the retrograde spread of a recombinant red fluorescent protein-expressing HRSV construct (rrHRSV)[8] from the site of inoculation. Although rrHRSV has previously been used to study the susceptibility of various cell types to virus infection in vitro,[8,36] our current report is the first wherein this biologic agent has been used to trace the route and extent of infection after intranasal instillation of virus in vivo. To establish the usefulness of our approach, immunohistochemistry and plaque assay were used to verify the sensitivity and specificity of fluorescence detected at 2, 3, 5, and 14 d after infection. By these combined methods, we were able to follow the retrograde spread of virus infection from the respiratory epithelium of the nasoturbinates and nasopharynx (at the earliest time point) to the Eustachian tubes and ethmoid turbinates at later time points. The ability to visualize the anatomy and kinetics of HRSV replication in the uppermost airway can now form the basis for future studies of upper-airway susceptibility to virus reinfection and bacterial coinfection.

## Materials and Methods

**Chinchillas.** Juvenile male and female chinchillas (*Chinchilla lanigera*; *n* = 12; weight, 347 ± 37 g; Rauscher Chinchilla Ranch, La Rue, OH) were included in this study. On the basis of physical examination by a licensed veterinarian, all animals were considered healthy upon arrival at our facility. Testing for specific pathogens was not performed. Animals were housed individually in a BSL 2 facility and were offered a commercial chinchilla pelleted chow and water ad libitum. Animals were acclimated for 7 to 10 d prior to challenge with rrHRSV. Video otoscopy and tympanometery revealed that all animals were free of middle ear disease at the time of rrHRSV challenge. All procedures used here were conducted humanely and have been described in detail elsewhere.[6] Animal housing and experimental procedures were approved by the Institutional Animal Care and Use Committee at the Research Institute at Nationwide Children's Hospital.

**Infection.** The rrHRSV was constructed and rescued as described previously.[8] Anesthetized chinchillas were challenged intranasally with $1 \times 10^7$ pfu rrHRSV delivered in 80 µL sterile PBS, with the total dose divided equally between nares. Three animals were euthanized on each of the following days after rrHRSV challenge: 2, 3, 5, and 14. Chinchillas were monitored by a licensed veterinarian daily after rrHRSV challenge for signs of clinical disease as well as by video otoscopy and tympanometry for signs of middle ear inflammation (otitis media).[6]

**Nasopharyngeal lavage and plaque assay.** Prior to euthanasia, chinchillas were anesthetized, and nasopharyngeal lavage fluids were collected as previously described.[6] Briefly, anesthetized prone chinchillas were allowed to passively inhale 500 µL sterile PBS in droplets delivered by sterile pipet tip. Nasopharyngeal lavage fluids were collected from the contralateral naris as they were exhaled and were stored at –80 °C. Viral titers in nasopharyngeal lavage fluids were determined by plaque assay performed as previously described.[6]

**Table 1.** Infectious rrHRSV in nasopharyngeal lavage fluids

| | Day 2 | Day 3 | Day 5 | Day 14 |
|---|---|---|---|---|
| *n* | 10 | 6 | 6 | 3 |
| mean | 8.1 | 21.2 | 5.8 | 0 |
| SEM | 4.1 | 16.1 | 3.9 | 0 |

Nasopharyngeal lavage fluids were recovered as indicated after intranasal infection of chinchillas with 1 x $10^7$ pfu rrHRSV. Viral load (x $10^3$ pfu rrHRSV/mL ) was determined by plaque assay. Virus load in the current study correlated with that found in nasopharyngeal lavage fluids from chinchillas challenged intranasally with the rrHRSV parent strain A2 (data not shown).

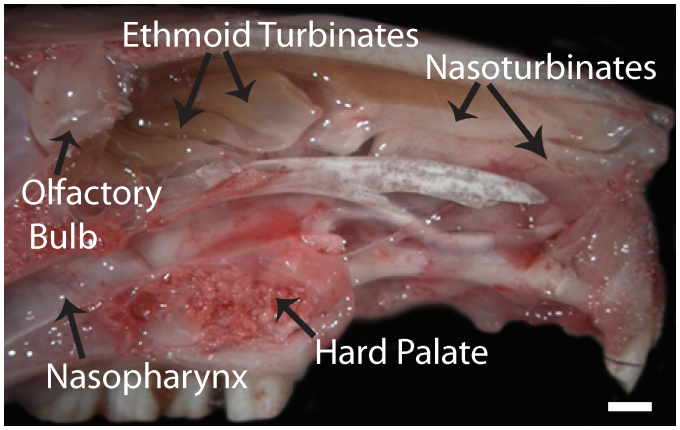


**Figure 1.** Gross anatomy of the chinchilla nasal cavity. Parasagittal section of an unfixed chinchilla head. The nasal cavity is composed of nasoturbinates rostrally, ethmoid turbinates caudally, and the nasopharynx ventrally. Bar, 5 mm.

**Confocal microscopy.** At euthanasia, the skull was sectioned in a sagittal plane after removal of extraneous tissues. Whole sagittal sections of the chinchilla head included the nasopharynx, naso- and ethmoid turbinates, and olfactory bulb. The Eustachian tube was dissected carefully away from the inferior bulla and then sectioned longitudinally. The middle ear was not examined in this study. The sagittal head and longitudinal Eustachian tube sections underwent confocal microscopy (LSM510 Meta laser module attached to an Axiovert 200M inverted microscope, Carl Zeiss, Thornwood, NJ). Thresholds were set by using uninfected chinchilla tissue and then were maintained for evaluation of rrHRSV-infected tissues to significantly reduce or eliminate the contribution of background fluorescence.

**Immunohistochemistry.** After confocal microscopic analysis, tissues were fixed in neutral buffered formalin and decalcified with 0.35 M EDTA in 0.1 M Tris (pH 6.95) until no calcium could be detected via chemical endpoint assay.[31] Decalcified tissues were paraffin-embedded, sectioned at 5 µm, and stained with hematoxylin and eosin or, for α-RSV immunohistochemistry, were incubated with goat polyclonal RSV antiserum (Biodesign, Saco, ME) diluted 1:500 in buffer followed by incubation with biotinylated rabbit antigoat antibody (ScyTek, Logan, UT). Virus detection was accomplished by means of a a streptavidin-horse radish peroxidase complex and aminoethyl carbazole as a chromagen (Scytek).

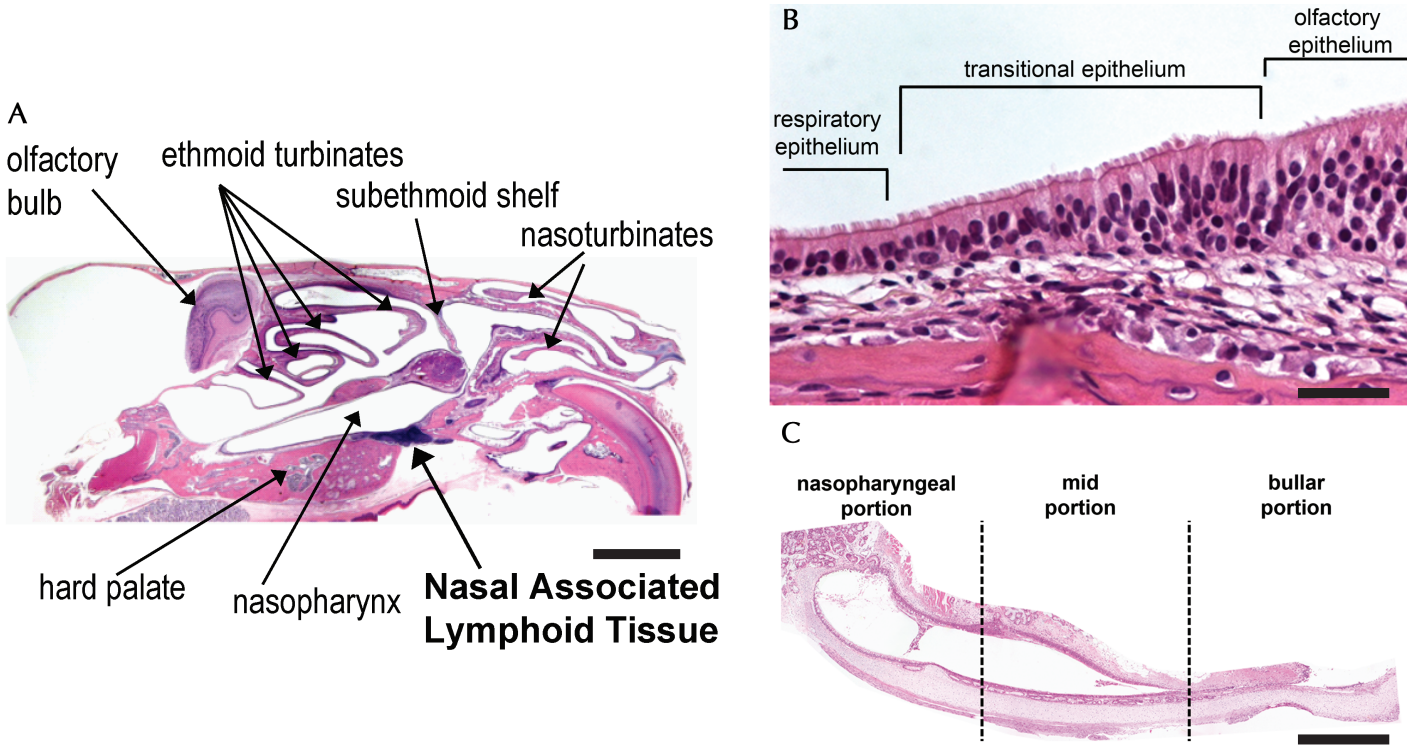


**Figure 2.** Microscopic anatomy of the chinchilla nasal cavity. (A) Chinchilla head, parasagittal section. The naso- and ethmoid turbinates are separated by the subethmoid shelf. (B) Ethmoid turbinate. The relatively sharp transition to olfactory epithelium is marked by the abrupt absence of cilia. (C) Eustachian tube, longitudinal section. RSV infection of the Eustachian tube begins at the nasopharyngeal opening and spreads retrograde toward the middle ear space as infection progresses. Hematoxylin and eosin stain; bar: 5 mm (A), 100 µm (B), 500 µm (C).

## Results

**Nasopharyngeal lavage fluids contain infectious virus.** Unlike the mouse model, wherein instillation of HRSV is generally intratracheal after intranasal delivery of 50 to 100 µL virus suspension, a similar volume containing $10^7$ pfu virus remains in the nasopharynx of chinchillas. We did not detect lower respiratory tract infection in chinchillas by plaque assay of lung homogenates after intranasal virus inoculation (data not shown).

We sought to assess both the path of virus infection in the chinchilla URT and the utility of the reagents available for these studies. To ensure that infection with rrHRSV was comparable to that observed with previously characterized RSV A2 strain,[6] viral load in NP lavage fluids collected on days 2, 3, 5, and 14 after virus instillation was determined by plaque assay (Table 1). In all but one animal, virus was detected in nasopharyngeal lavage fluids by this method at one or more time points after HRSV challenge. Virus was found in nasopharyngeal lavage fluids on days 2, 3 and 5 after rrHRSV challenge but had cleared by day 14. Viral titers were not measured in all animals at all time points to avoid repeated exposure to anesthesia.

**Gross and microscopic anatomy of the chinchilla nasal cavity.** The nasal cavity of the chinchilla is composed of the naso- and ethmoid turbinates rostrally and caudally, respectively, and the nasopharynx ventrally (Figures 1 and 2 A). The nasoturbinates form the rostral-most portion of the nasal cavity and are composed of thin scroll-like bones lined by ciliated columnar respiratory epithelium interspersed with goblet cells. The ethmoid turbinates form the caudalmost portion of the nasal cavity and, like the nasoturbinates, are composed of thin scroll-like bones. The ethmoid turbinates, however, are lined predominantly by olfactory epithelium, but regions with respiratory and transitional epithelium are also present. The olfactory epithelium is composed of neuronal cell bodies and processes, superficial nonciliated sustentacular cells, which cover the neuronal cell bodies and surround their processes, as well as the ducts from the submucosal Bowman glands. Figure 2 B is centered on the ethmoid turbinate mucosa and demonstrates the transition from respiratory to olfactory epithelium. The respiratory epithelium just before the transition consists of tall columnar ciliated cells as well as basal cells. The relatively sharp transition between these epithelial types is marked in Figure 2 B but can be easily appreciated by noting the abrupt absence of cilia. The nasopharynx connects the nasal cavity to the middle and lower respiratory tracts and is lined by ciliated columnar respiratory epithelium with interspersed goblet cells. The Eustachian tube, a tubal organ, connects the nasopharynx and the middle ear space. The mucosal surface of the Eustachian tube is lined by ciliated columnar epithelial cells interspersed with goblet cells proximally and transitions to low columnar to squamoid nonglandular nonciliated epithelium distally (Figure 2 C).[26]

**Expression of red fluorescent protein marks the sites and progression of RSV infection.** On day 2 after challenge with rrHRSV, the time point at which fluorescence was most intense at this site, red fluorescence was detected along the entire length of the nasopharynx (Figure 3). Fluorescence was present as far retrograde as the nasoturbinates at this time but had not yet reached the ethmoid turbinates (Figure 4). By 3 d after challenge, the distribution of red fluorescence had expanded to involve all areas of the

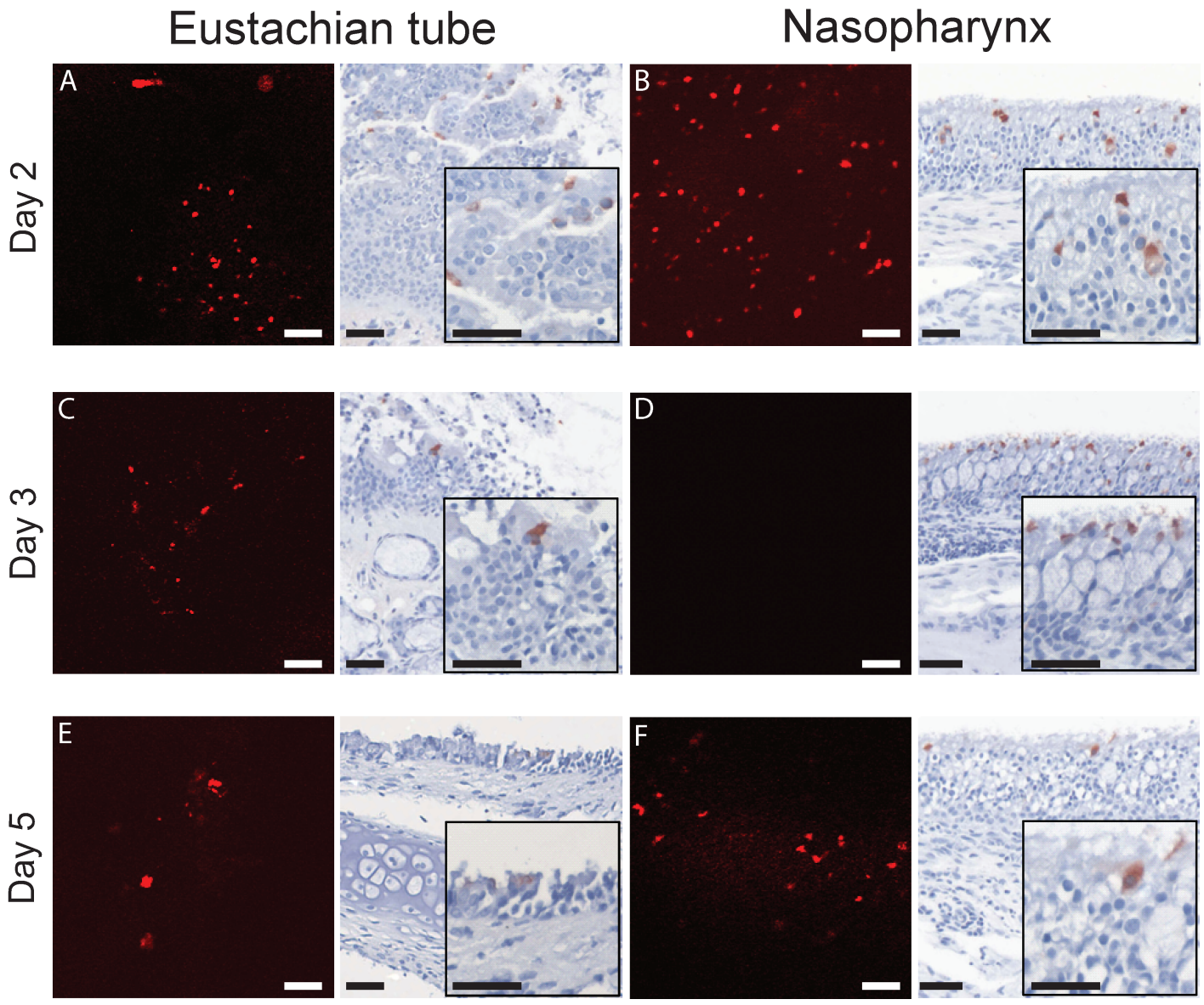


**Figure 3.** Eustachian tube and nasopharynx of rrHRSV-infected animals, confocal microscopy and immunohistochemistry. Multifocal punctate red fluorescence was detected in the proximal portion of the Eustachian tube on days 2 and 3 (A, C) and in the distal portion of the Eustachian tube on day 5 (E). Multifocal to widespread punctate red fluorescence was detected in the nasopharynx on days 2 (B) and 5 (F) and was most intense on day 2. HRSV-infected cells were not detected at these sites by confocal microscopy or immunohistochemistry on day 14 (not shown). The degree and location of RSV infection determined by using these 2 detection methods were highly correlative. The single exception was the nasopharynx on day 3 (D), in which red fluorescence was absent whereas clusters of RSV infected cells were detected by immunohistochemistry. Insets depict increased magnification of the same field. Immunohistochemistry and confocal microscopy of sham-infected (saline only) chinchillas were negative in all sections examined (data not shown). Bar, 100 µm.

nasal cavity (Figures 3 C and 4 C, D), except for the nasopharynx, which was positive on days 2 and 5 (Figure 3 B, D, and F). Red fluorescence on day 5 was similar in intensity and distribution to that observed on day 3 but was more intense in the ethmoid turbinates as the infection progressed (Figure 4).

To determine the kinetics of ascension of rrHRSV from the nares to the proximal (nasopharyngeal) and distal (bullar) Eustachian tube openings, we analyzed these structures. Red fluorescence was present at the proximal orifice to the midpoint of the Eustachian tube by day 2 (Figure 3 A) and had progressed to the distal portion of the Eustachian tube by day 5 (Figure 3 E). Fluorescence was not detected in any portion of the nasal cavity or Eustachian tube on day 14 after HRSV challenge, the latest time point examined in this study.

There was remarkable consistency of virus infection kinetics between animals, with rapid spread of infection from the nasopharynx to the nasoturbinates, proximal Eustachian tube, and then to the distal Eustachian tube and ethmoid turbinates. In addition, rrHRSV continues to replicate in the chinchilla naso- and ethmoid turbinates after it is largely cleared from the nasopharynx. Although the human nasal cavity is much less complex than

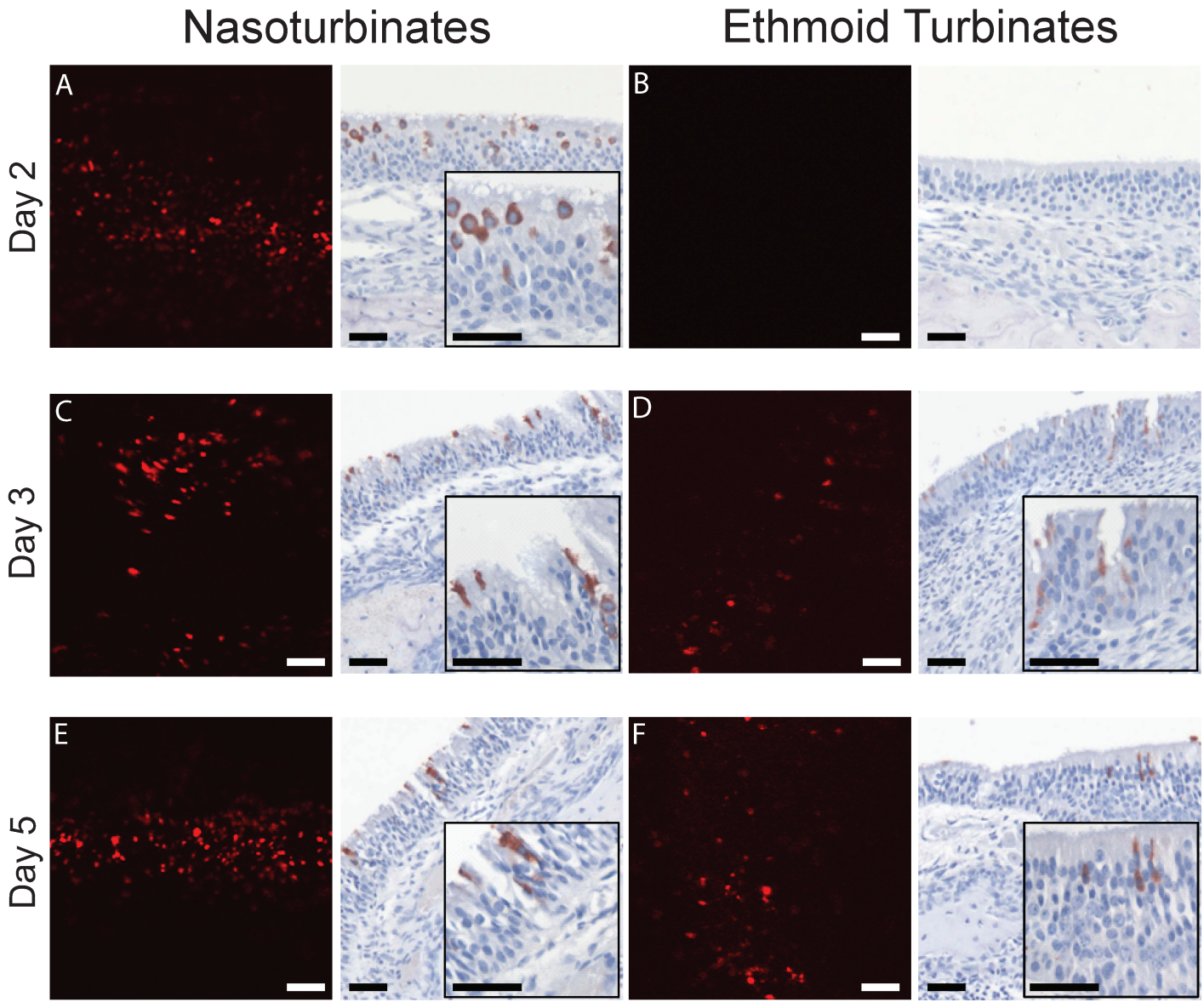


**Figure 4.** Naso- and ethmoid turbinates of rrHRSV-infected animals, confocal microscopy and immunohistochemistry. Widespread punctuate red fluorescence was detected throughout the nasoturbinates at similar intensity on days 2 (A), 3 (C), and 5 (E). Neither red fluorescence (B) nor immunopositive cells (D) were detected in the ethmoid turbinates on day 2. However, by day 3 (D) and increasing in intensity by day 5 (F), multifocal punctate red fluorescence as well as immunopositive cells were detected at this anatomic site. HRSV-infected cells were not seen by confocal microscopy on day 14 (not shown). Insets depict increased magnification of the same field. Bar, 100 µm.

that of chinchilla, HRSV may persist in permissive locations in humans as well.

**Confirmation of RSV infection by immunohistochemistry.** Unlike fluorescent imaging, immunohistochemistry offers an opportunity to determine the specific cell types infected within the upper airway and is thus an essential adjunct to confocal microscopy. Immunohistochemical labeling and confocal microscopic analysis of the Eustachian tube and the decalcified nasal cavity of rrHRSV-infected chinchillas produced similar results, with multiple small foci of virus infection detected with both techniques. Compared with confocal imaging, immunohistochemistry was slightly more sensitive, in that small clusters of antigen positive cells were found in the nasopharynx and nasoturbinate 3 d (Figure 3) and in the ethmoid turbinate 14 d (Figure 5) after infection, in the absence of a fluorescent signal. These data indicate that use of red fluorescent protein-expressing HRSV is a valid method for tracing the spread of infection but also demonstrate the importance of the complementary histologic information provided by immunohistochemistry.

Taken together, our data show that the red fluorescence observed by confocal microscopy was in fact due to the presence of intracellular rrHRSV protein expression in all types of mucosal epithelium in the nasal cavity, including tall, ciliated, pseudostratified respiratory epithelium, transitional epithelium, and olfactory epithelium (Figures 4 F and 5). The ciliated respiratory epithelium is thought to be the primary target for RSV in the human host,[15,36]

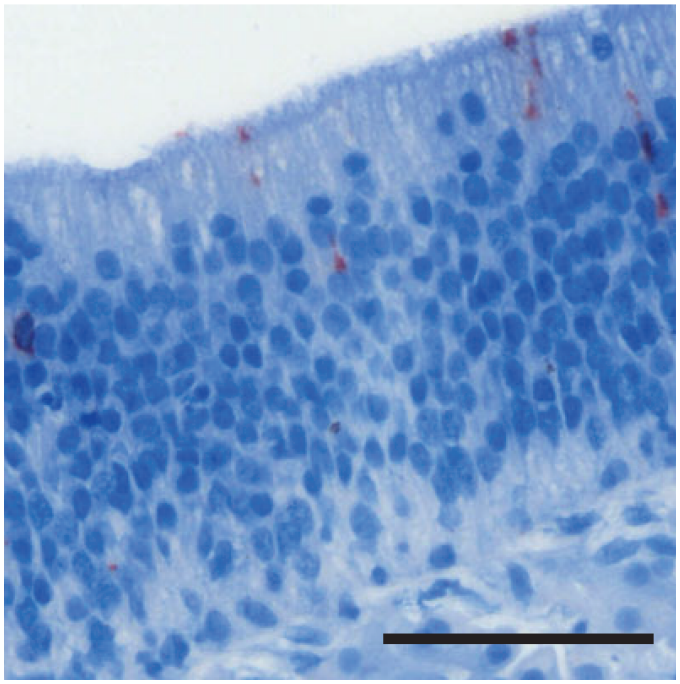

**Figure 5.** Ethmoid turbinate 14 d after rrHRSV infection, immunohistochemistry. Although red fluorescence was not detected at any site on day 14, occasional immunopositive cells were observed in the ethmoid (as shown) or nasoturbinates (not shown) of 2/3 of animals at this time point, suggesting that the nasal cavity may serve as a site for prolonged HRSV replication in chinchillas. Bar, 100 µm.

but because nasal epithelium from infected patients is not examined in the course of routine medical practice, whether human olfactory epithelium is susceptible to RSV infection is unknown. We have previously described RSV-infected olfactory neurons in BALB/c mice,[6] and we confirm here that olfactory epithelium is also a target for RSV infection in chinchillas. Although specific markers for each cell type are not available for chinchillas, the RSV-infected cells within the olfactory mucosa are morphologically most consistent with neuronal cell bodies and processes.

## Discussion

Our interest in modeling upper airway infection with RSV arises from our interest in the pathogenesis of otitis media. Chinchillas, rats, gerbils, and hamsters have been used to experimentally model human otitis media;[23] however, to date only in chinchillas and ferrets[24] has it been possible to demonstrate the polymicrobial nature of otitis media, which always involves bacterial superinfection of a virus-compromised upper airway. Development of the first viral-bacterial superinfection model of otitis media contributed to our understanding of the mechanisms by which influenza A virus predisposes to secondary invasion of the chinchilla middle ear by *Streptococcus pneumonia*,[2-4] and our laboratory has used the chinchilla model similarly to study adenovirus-mediated predisposition to nontypeable *Hemophilus influenzae* of the Eustachian tube.[1] However, despite its predominance as a copathogen of this highly prevalent pediatric disease, HRSV infection of the URT and its association with bacterial otitis media has not been well studied.

Our limited understanding of URT infection by RSV is largely due to lack of a relevant animal model in which to explore questions regarding RSV pathogenesis in the Eustachian tube and middle ear (tubotympanum). In an attempt to develop such a model, we have characterized HRSV infection of the uppermost airway in both murine and chinchilla hosts[6] challenged in a manner designed to restrict viral delivery to the nasal cavity without dose-loss to either the gastrointestinal tract or lungs.[35] In the cited study, chinchillas proved to be more permissive to upper-airway infection than were BALB/c mice, in which infection largely was restricted to the lungs.[6] In chinchillas, as in human hosts, HRSV is primarily an upper-airway infection, and in the current study, we have used a variety of tools to map the anatomy of URT infection by this virus. Although chinchillas did not develop signs of clinical disease at any time during the study period, microscopic examination of nasal mucosa revealed mild multifocal neutrophilic and lymphocytic infiltrates (data not shown).

HRSV spread from the site of inoculation to the pharyngeal orifice of the Eustachian tube by 48 h after challenge in chinchillas, but 5 d were required before virus could be detected in the distalmost aspect of the Eustachian tube. Virus was present in the nasoturbinates (equivalent to the human concha) 2 d after challenge and as far retrograde as the ethmoid turbinates by day 3. Immunohistochemistry allowed us to determine the microanatomy of infection, revealing not just the location of infected cells but also the cell types infected. In general, as has been reported for well-differentiated, polarized, pseudostratified human airway epithelial cells that grow at the air-liquid interface,[36] infection was limited to ciliated respiratory epithelial cells in chinchillas. However, in the ethmoid turbinates, immunopositive cells were identified within olfactory as well as respiratory epithelial mucosa. Although there are no reports of olfactory epithelial infection by RSV in human subjects, we previously observed this localization in BALB/c mice, wherein we demonstrated foci of RSV antigen-positive cells in ductal epithelium as well as in bipolar neurons of the olfactory epithelium.[6] In the current study, we also observed infection of bipolar neurons within the olfactory epithelium, demonstrating susceptibility of that cell type to infection in a second rodent species.

Viral clearance of rrHRSV, as measured by plaque assay and confocal microscopy, was complete by 5 d after infection, although clusters of immunopositive epithelial cells were still present in sections taken from the nasoturbinates and ethmoid turbinates on day 14. This result suggests that low-level upper-airway infection continues beyond the observation period of the present study, and we currently are exploring the possibility of long-term persistence at this site. Given the annual appearance of RSV in the absence of a known animal reservoir, it is certainly possible that some persons may serve as persistently infected carriers. Although the site(s) of persistent infection in the mouse are unknown, viral genomic RNA and mRNA were detected in lung homogenates from BALB/c mice that had been challenged intranasally with HRSV more than 100 d earlier.[30] The ease with which persistently infected primary human airway epithelial[36] and dendritic cell[14] cultures have been established also supports the idea that persistent HRSV infection in the absence of cytopathology may be possible, but an in vivo source of persistently infected cells has not yet been identified. Our previous demonstration of infected olfactory neurons and the identification of antigen-positive

neurons in infected mouse lungs[20] suggests another possible virus reservoir.

In conclusion, unlike the relatively resistant BALB/c mouse, the more susceptible chinchilla likely will prove to be a useful model for studies of RSV infection of the upper airway. Now that the kinetics of Eustachian tube compromise by the virus have been established, we can explore both bacterial superinfection in that compartment as well as the mechanisms by which HRSV infection allows middle ear invasion by bacterial organisms that are normally nonpathogenic including nontypeable *Haemophilus influenza* and *Moraxella catarrhalis*. In addition, the chinchilla model of URT infection provides a new platform to address host defense mechanisms against reinfection, including why these defenses are inadequate in the case of HRSV.

## Acknowledgments

We thank Sara Mertz for assistance with immunohistochemistry, Barbara Newton for excellent technical assistance in constructing rrHRSV (BN1), and Jennifer Neelans for manuscript preparation. This work was supported by grant R01 DC006468 from the National Institute of Diabetes and Chronic Disease, NIH, to JED and LOB and grant R01 DC03915 from the National Institute of Diabetes and Chronic Disease, NIH, to LOB.

## References

1. **Bakaletz LO, Daniels RL, Lim DJ.** 1993. Modeling adenovirus type 1-induced otitis media in the chinchilla: effect on ciliary activity and fluid transport function of Eustachian tube mucosal epithelium. J Infect Dis **168:**865–872.
2. **Giebink GS, Berzins IK, Marker SC, Schiffman G.** 1980. Experimental otitis media after nasal inoculation of *Streptococcus pneumoniae* and influenza A virus in chinchillas. Infect Immun **30:**445–450.
3. **Giebink GS, Ripley ML, Wright PF.** 1987. Eustachian tube histopathology during experimental influenza A virus infection in the chinchilla. Ann Otol Rhinol Laryngol **96:**199–206.
4. **Giebink GS, Wright PF.** 1983. Different virulence of influenza A virus strains and susceptibility to pneumococcal otitis media in chinchillas. Infect Immun **41:**913–920.
5. **Girard MP, Cherian T, Pervikov Y, Kieny MP.** 2005. A review of vaccine research and development: human acute respiratory infections. Vaccine **23:**5708–5724.
6. **Gitiban N, Jurcisek JA, Harris RH, Mertz SE, Durbin RK, Bakaletz LO, Durbin JE.** 2005. Chinchilla and murine models of upper respiratory tract infections with respiratory syncytial virus. J Virol **79:**6035–6042.
7. **Graham BS, Perkins MD, Wright PF, Karzon DT.** 1988. Primary respiratory syncytial virus infection in mice. J Med Virol **26:**153–162.
8. **Guerrero-Plata A, Casola A, Suarez G, Yu X, Spetch L, Peeples ME, Garofalo RP.** 2006. Differential response of dendritic cells to human metapneumovirus and respiratory syncytial virus. Am J Respir Cell Mol Biol **34:**320–329.
9. **Hall CB.** 2001. Respiratory syncytial virus and parainfluenza virus. N Engl J Med **344:**1917–1928.
10. **Hall CB, Walsh EE, Long CE, Schnabel KC.** 1991. Immunity to and frequency of reinfection with respiratory syncytial virus. J Infect Dis **163:**693–698.
11. **Heikkinen T**. 2000. Role of viruses in the pathogenesis of acute otitis media. Pediatr Infect Dis J **19:**S17–S22; discussion S22–S23.
12. **Heikkinen T, Thint M, Chonmaitree T.** 1999. Prevalence of various respiratory viruses in the middle ear during acute otitis media. N Engl J Med **340:**260–264.
13. **Henderson FW, Collier AM, Sanyal MA, Watkins JM, Fairclough DL, Clyde WA Jr, Denny FW.** 1982. A longitudinal study of respiratory viruses and bacteria in the etiology of acute otitis media with effusion. N Engl J Med **306:**1377–1383.
14. **Hobson L, Everard M.** 2008. Persistent of respiratory syncytial virus in human dendritic cells and influence of nitric oxide. Clin Exp Immunol **151:**359–366.
15. **Johnson JE, Gonzales RA, Olson SJ, Wright PF, Graham BS.** 2007. The histopathology of fatal untreated human respiratory syncytial virus infection. Mod Pathol **20:**108–119.
16. **Johnston SL, Pattemore PK, Sanderson G, Smith S, Campbell MJ, Josephs LK, Cunningham A, Robinson BS, Myint SH, Ward ME, Tyrrell DA, Holgate ST.** 1996. The relationship between upper respiratory infections and hospital admissions for asthma: a time–trend analysis. Am J Respir Crit Care Med **154:**654–660.
17. **Klein BS, Dollete FR, Yolken RH.** 1982. The role of respiratory syncytial virus and other viral pathogens in acute otitis media. J Pediatr **101:**16–20.
18. **Klein JO, Teele DW.** 1976. Isolation of viruses and mycoplasmas from middle ear effusions: a review. Ann Otol Rhinol Laryngol **85:**140–144.
19. **Korppi M, Leinonen M, Koskela M, Makela PH, Launiala K.** 1989. Bacterial coinfection in children hospitalized with respiratory syncytial virus infections. Pediatr Infect Dis J **8:**687–692.
20. **Li XQ, Fu ZF, Alvarez R, Henderson C, Tripp RA.** 2006. Respiratory syncytial virus (RSV) infects neuronal cells and processes that innervate the lung by a process involving RSV G protein. J Virol **80:**537–540.
21. **Monobe H, Ishibashi T, Nomura Y, Shinogami M, Yano J, Kaga K.** 2002**.** Detection of various respiratory virus genomic sequences in middle ear fluids in children with acute otitis media and its relationship to the prognosis [abstract]. Twenty-Fifth Annual Midwinter Research Meeting, Association for Research in Otolaryngology. St Petersburg Beach, Florida, 27–31 January 2002. Proc Assoc Res Otolaryngol **25:**222.
22. **Moore ML, Peebles RS Jr.** 2006. Respiratory syncytial virus disease mechanisms implicated by human, animal model, and in vitro data facilitate vaccine strategies and new therapeutics. Pharmacol Ther **112:**405–424.
23. **Openshaw PJ, Tregoning JS.** 2005. Immune responses and disease enhancement during respiratory syncytial virus infection. Clin Microbiol Rev **18:**541–555.
24. **Peltola VT, Boyd KL, McAuley JL, Rehg JE, McCullers JA.** 2006. Bacterial sinusitis and otitis media following influenza virus infection in ferrets. Infect Immun **74:**2562–2567.
25. **Pitkaranta A, Virolainen A, Jero J, Arruda E, Hayden FG.** 1998. Detection of rhinovirus, respiratory syncytial virus, and coronavirus infections in acute otitis media by reverse transcriptase–polymerase chain reaction. Pediatrics **102:**291–295.
26. **Prince GA, Jenson AB, Horswood RL, Camargo E, Chanock RM.** 1978. The pathogenesis of respiratory syncytial virus infection in cotton rats. Am J Pathol **93:**771–791.
27. **Rafiefard F, Johansson B, Tecle T, Orvell C.** 2004. Molecular epidemiology of respiratory syncytial virus (RSV) of group A in Stockholm, Sweden, between 1965 and 2003. Virus Res **105:**137–142.
28. **Ruuskanen O, Arola M, Putto-Laurila A, Mertsola J, Meurman O, Viljanen MK, Halonen P.** 1989. Acute otitis media and respiratory virus infections. Pediatr Infect Dis J **8:**94–99.
29. **Sarkkinen H, Ruuskanen O, Meurman O, Puhakka H, Virolainen E, Eskola J.** 1985. Identification of respiratory virus antigens in middle ear fluids of children with acute otitis media. J Infect Dis **151:**444–448.
30. **Schwarze J, O'Donnell DR, Rohwedder A, Openshaw PJ.** 2004. Latency and persistence of respiratory syncytial virus despite T cell immunity. Am J Respir Crit Care Med **169:**801–805.
31. **Seilly DJ.** 1982. A chemical test to determine the end point of EDTA decalcification. Med Lab Sci **39:**71–73.
32. **Sikkel MB, Quint JK, Mallia P, Wedzicha JA, Johnston SL.** 2008. Respiratory syncytial virus persistence in chronic obstructive pulmonary disease. Pediatr Infect Dis J **27:**S63–S70.

33. **Sullender WM.** 2000. Respiratory syncytial virus genetic and antigenic diversity. Clin Microbiol Rev **13:**1–15.
34. **Uhari M, Hietala J, Tuokko H.** 1995. Risk of acute otitis media in relation to the viral etiology of infections in children. Clin Infect Dis **20:**521–524.
35. **Visweswaraiah A, Novotny LA, Hjemdahl-Monsen EJ, Bakaletz LO, Thanavala Y.** 2002. Tracking the tissue distribution of marker dye following intranasal delivery in mice and chinchillas: a multifactorial analysis of parameters affecting nasal retention. Vaccine **20:**3209–3220.
36. **Zhang L, Peeples ME, Boucher RC, Collins PL, Pickles RJ.** 2002. Respiratory syncytial virus infection of human airway epithelial cells is polarized, specific to ciliated cells, and without obvious cytopathology. J Virol **76:**5654–5666.